Structural Chemistry (2021) 32:1529–1539
https://doi.org/10.1007/s11224-021-01728-8

ORIGINAL RESEARCH

A comparative study of interplay effects between the cation-π and intramolecular hydrogen bond interactions in the various complexes of methyl salicylate with Mn^{+}, Fe^{2+}, Co^{+}, Ni^{2+}, Cu^{+}, and Zn^{2+} cations

Mahsa Pirgheibi[1] · Marziyeh Mohammadi[1] · Azadeh Khanmohammadi[2]

Received: 19 October 2020 / Accepted: 10 January 2021 / Published online: 18 January 2021

Abstract

The interplay among two important noncovalent interactions involving aromatic ring is studied by means of density functional theory (DFT) calculations on complexes of methyl salicylate with Mn^{+}, Fe^{2+}, Co^{+}, Ni^{2+}, Cu^{+}, and Zn^{2+} cations. The energetic, geometrical, spectroscopic, topological, and molecular orbital descriptors are applied to evaluate the strength of the cation-π and intramolecular hydrogen bond (IMHB) interactions. These outcomes are compared with the parent molecule of methyl salicylate and the corresponding results of benzene (BEN) complexes with the cited cations as a set of reference points. Based on the energetic conclusions, for the double-charge cations, the simultaneous presence of these interactions enhances the strength of the cation-π, while for the mono-charge cations, the reverse process is observed. On the other hand, for both type of the cations (mono- and double-charge), the coupling of noncovalent interactions reduces the strength of the IMHB in the studied systems. The computations in this study are discussed with the Bader theory of atoms in molecules (AIM), the natural bond orbital (NBO) analysis, and the frontier molecular orbital (FMO) theory.

Keywords Cation π · Intramolecular hydrogen bond · DFT · AIM · NBO

Introduction

Methyl salicylate (MS) is known chemically as 2-(methoxycarbonyl) phenol, which has the empirical formula $C_8H_8O_3$. It is employed as the major component of a fully definable essential oil (oil of wintergreen). MS may be characterized as a colorless, yellowish, or reddish, oily liquid with the distinct odor and taste of wintergreen or gaultheria. It is used in cosmetics as warming-up agent and also applied in perfumery as a modifier in blossom fragrance and as a mild antiseptic in oral hygiene products [1]. MS has anti-inflammatory properties [2]. For acute joint and muscular pain, MS is used as a rubefacient and analgesic in deep heating liniments [3]. It relieves musculoskeletal pain in the muscles, joints, and tendons by causing irritation and reddening of the skin due to dilated capillaries and increased blood flow [4]. No studies have been performed with the primary purpose of determining the carcinogenicity of MS.

Noncovalent interactions (NCIs) such as hydrogen bond, cation-π, anion-π, and other weak forces govern the organization of multicomponent supramolecular assemblies [5–10].The hydrogen bond (HB), as a popular form of NCIs, is a unique interaction whose importance is great in chemical and bio-chemical reactions including life processes [11]. It is an attractive interaction between a proton donor X–H and a proton acceptor Y in the same or in a different molecule (X-H···Y). According to the conventional definition, H atom is bonded to electronegative atoms such as N, O, and F. Y is either an electronegative region or a region of electron excess [11–16]. Among various types of interactions, the influence of π-electron delocalization on HB interactions plays a special

✉ Marziyeh Mohammadi
m.mohammadi@vru.ac.ir

[1] Department of Chemistry, Faculty of Science, Vali-e-AsrUniversity of Rafsanjan, P. O. Box: 77176, Rafsanjan, Iran

[2] Department of Chemistry, Payame Noor University, P. O. BOX 19395-3697, Tehran, Iran

role [11, 12]. This effect is called resonance-assisted hydrogen bonds (RAHBs) [17]. It seems that for stronger RAHBs, the delocalization becomes more important, and the electrostatic interaction energy is less significant than for weaker. This may be a common characteristic of HBs.

The cation-π interaction, as another ensemble of NCIs, implies the electrostatic attraction between ionic species and the induced dipole of the aromatic moiety [18]. The magnitude of the cation-π interaction is proposed to depend on the nature of both the aromatic and cationic groups involved. The cation-π interaction is in general dominated by electrostatic and cation-induced polarization [19]. Dispersive and hydrophobic forces are thought to act in support of this type of association [20]. The significance of cation-π interactions in the design of organic nanotubes, ionophores, and models for biological receptors has been clearly demonstrated [21–26].

The interplay between the NCIs that are ubiquitous in biological systems may be important in many areas of the supramolecular chemistry, molecular recognition, catalysis, and crystal engineering [27, 28]. The importance of NCIs involving aromatic systems and the interplay among them can lead to synergetic effects. In the last decades, the different studies have been performed on the interplay effects between the HB and cation-π interactions. For the first time, the mutual effect of intermolecular HB and cation-π interactions in several model systems has been extensively studied by Frontera et al. [29–31], and the synergetic effects were observed. In 2008, Vijay et al. reported the strong cooperativity between cation-π interaction involving alkali and alkaline earth metal ions, π-π, and HB interactions [32]. Also, the interplay between cation-π and HB interactions was studied in different systems with quantum chemical calculations by Li et al. [33]. Hence, the interplay between these interactions in the present study can be important and might help to understand some biological processes.

In the present letter, it should be mentioned that the investigated cations are selected to have closed-shell electronic configuration. In fact, the cations are preferred to be mono- or divalent, because higher oxidation states could lead to very disparate results. Metal ions play a key role in wide ranging biological processes, such as the regulation of enzyme, stabilization, and function of nucleic acids [34, 35].With the biological importance of these ions, it is important to study complexation with bioactive ligands to understand functions of their complexes and to find new bioactive compounds. The goal of the current research is to analyze a comparative study of interplay effects between the cation-π and IMHB interactions in the various complexes of MS with Mn^{+}, Fe^{2+}, Co^{+}, Ni^{2+}, Cu^{+}, and Zn^{2+} cations. The geometrical parameters, binding energies, and topological properties are examined to gain further insight into the effects of these interactions on each other. For this study, DFT calculations are done, and the AIM and NBO analyses are exploited. Finally, a complete investigation of these interactions is presented on molecular orbital (MO) data in the studied complexes.

Computational methods

All of the calculations in the present study are performed using the Gaussian 03 [36] set of program. The structures are optimized with the DFT method using the M06-2X functional [37] along with the M06-2X/aug-cc-pVTZ basis set [38]. Frequency calculations are carried out to prove that the resulting stationary points are real energy minima. For the studied complexes, the binding energies ($\Delta E_{ion\text{-}\pi}$) are calculated by evaluating the difference between the total energies of complex and the optimized energies of monomers, as given in Eq. (1):

$$\Delta E_{ion-\pi} = E_{cation-\pi} - \left(E_{cation} + E_{\pi-system}\right) \quad (1)$$

where $E_{cation-\pi}$ is the total energy of complex and E_{cation} and $E_{\pi\text{-}system}$ are the energies of the relaxed cation and MS (or BEN) monomer, respectively. The obtained binding energies are corrected for the basis set superposition error (BSSE) using counterpoise correction method of Boys and Bernardi [39].The topological electron charge density is analyzed by the atoms in molecules (AIMs) method [40, 41], using the AIM2000 program [42]. The achieved wave functions at the M06-2X/aug-cc-pVTZ computational level are also applied to calculate the orbital interaction and the charge transfers within the NBO framework [43] using the NBO program [44] under Gaussian 03 package. The molecular orbital (MO) calculations are performed on the investigated complexes with the same level of DFT theory. Finally, electronic descriptors such as energy gap, softness (S), chemical hardness (η) [45], electronic chemical potential (μ) [46], electrophilicity index (ω) [47], and electronegativity (χ) [48] are calculated as defined in Eqs. (2), (3), (4), and (5) according to Koopmans theorem [49] to investigate the local characteristics of the complexes:

$$\mu = \left(\frac{\partial E}{\partial N}\right)_{V(r),T} \quad (2)$$

$$\eta = \left(\frac{\partial^2 E}{\partial N^2}\right)_{V(r),T} \quad (3)$$

$$S = \frac{1}{2\eta} \quad (4)$$

$$\omega = \frac{\mu^2}{2\eta} \quad (5)$$

Results and discussions

Energetic descriptors

In the current research, the mutual influences of the cation-π and IMHB interactions are investigated on the different binary complexes of MS with (M = Mn^{+}, Fe^{2+}, Co^{+}, Ni^{2+}, Cu^{+}, and Zn^{2+}) cations as the benchmark systems. In addition, for deeper understanding the nature of mentioned interactions, it is necessary to compare the results of the titled complexes with the appropriate references, such as the parent molecule (MS) and the BEN···M complexes. The considered complexes are illustrated according to the position of the metal cations (M) on the benzene ring (see Fig. 1). The values of the calculated binding energies without and with the BSSE correction (ΔE and ΔE_{BSSE}) are demonstrated in Table 1. For the MS···M and BEN···M complexes, the interaction strength based on the calculated binding energies is as follows:

$$\pi\bullet\bullet\bullet Ni^{2+} > \pi\bullet\bullet\bullet Fe^{2+} > \pi\bullet\bullet\bullet Zn^{2+} > \pi\bullet\bullet\bullet Mn^{+} > \pi\bullet\bullet\bullet Co^{+} > \pi\bullet\bullet\bullet Cu^{+}$$

As can be seen, the divalent complexes show the strongest interactions, whereas the weakest those belong to the monovalent ones. By comparison of the binding energies of the corresponding complexes of the MS and BEN (Table 1), it is found that the presence of RAHB ring increases the strength of cation-π interaction in divalent complexes. The reverse behavior is observed for the cation-π interactions in monovalent complexes. These results are strongly dependent on the nature of metal cations. Since cation-π interactions are predicted by electrostatics, it follows that cations with larger charge density interact more strongly with π systems. In the studied complexes, it can be seen that the divalent cations carry the most positive charge, whereas the least positive charge exists on the monovalent ones. This result leads to transfer some electron density of the RAHB units to the benzene ring that increases strength of cation-π interaction in these systems. In contrast, the greater ionic radius and lengthening of the metal–benzene distance of the monovalent complexes with respect to divalent ones are factors that may cause weakening of the cation-π interaction in these structures.

In this exploration, the approximate values of the IMHB energies of RAHB systems are calculated by the Espinosa and Molins method [50]. Herein, the HB energies (E_{HB}) could be estimated from the properties of bond critical points. The simple relationship between HB energy and the potential energy density $V(r_{cp})$ at the critical point corresponding to O···H contact is assigned to be $E_{HB} = 1/2\ V(r_{cp})$ [50–52]. Inspection of our theoretical results reveals that with the exception of MS···Ni^{2+} complex, the values of IMHB energy are lower than the parent molecule. This denotes that the presence of cation-π interaction decreases the IMHB strength. The electron density decrease within the RAHB units may be related to the attractive effects between the cations and π-electrons of the benzene ring. Hence, the reduced IMHB energies are found to be in the order MS···Co^{+} (0.74) > MS···Mn^{+} (0.54) > MS···Cu^{+} (0.27 kcal mol^{-1}) and MS···Zn^{2+} (0.52) > MS···Fe^{2+} (0.12 kcal mol^{-1}) for the corresponding complexes (see Table 1).

It is worth mentioning that, in the Ni^{2+} complex, after geometry optimization, the cation does not remain exactly along the perpendicular symmetric axis of benzene ring and approaches little to the ring bonds. It seems that the deviation of cation from the symmetric axis of the benzene ring can be related to the more negative electronic charge of ring C–C bond. Besides, in the Ni^{2+} complex, due to the strong cation-π interaction causing the architecture of "binary-system moiety" distortion, so that, the presence of RAHB unit destroys a little bit the aromaticity of the benzene ring, and this makes the cation-π interaction less efficient [53, 54]. Hence, with the merging of the RAHB unit and the benzene ring, the aromaticity of the benzene ring slightly decreases. This causes that the π-electron delocalization between the benzene ring and the RAHB unit also reduce. Thus, the less charge transfer from the RAHB unit to the benzene ring leads to the increment of HB strength in this system. For the Ni^{2+} complex, it can be observed that, in general, both cation-π and HB interactions have similar trend for the ΔE_{BSSE} and E_{HB} values, indicating that the effect of HB on the cation-π interaction is similar to the effect of the cation-π interaction on HB. Therefore, the

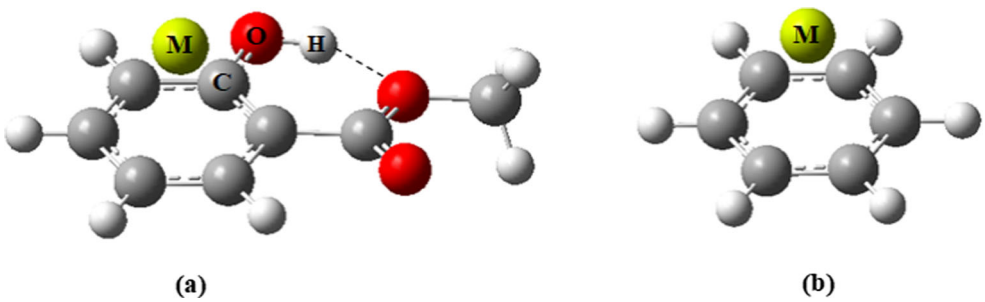

Fig. 1 Molecular structures of (**a**) MS···M and (**b**) BEN···M complexes (M = Mn^{+}, Fe^{2+}, Co^{+}, Ni^{2+}, Cu^{+}, Zn^{2+})

Table 1 The BSSE-corrected binding and IMHB energies (ΔE_{BSSE} and E_{HB}, in kcal mol^{-1}), the geometrical (bond lengths (d), in Å, and bond angles (θ), in °), and spectroscopic descriptors (ν, in cm^{-1}) of complexes calculated at the M06-2X/aug-cc-pVTZ level of theory

	ΔE_{BSSE}	$d_{\pi\cdots M}$	$\nu_{\pi\cdots M}$	E_{HB}	$d_{O\text{-}H}$	$d_{H\cdots O}$	θ_{OHO}	$\nu_{O\text{-}H}$
BEN···Ni^{2+}	−197.72	1.776	302.0	–	–	–	–	–
BEN···Fe^{2+}	−173.58	1.693	324.4	–	–	–	–	–
BEN···Zn^{2+}	−162.79	1.806	304.5	–	–	–	–	–
BEN···Mn^{+}	−93.58	1.601	329.9	–	–	–	–	–
BEN···Co^{+}	−66.19	1.767	241.8	–	–	–	–	–
BEN···Cu^{+}	−53.15	1.930	217.1	–	–	–	–	–
MS	–	–	–	−10.09	0.967	1.803	141.7	3746.8
MS···Ni^{2+}	−213.69	1.841	347.6	−13.83	0.998	1.703	142.2	3214.2
MS···Fe^{2+}	−186.76	1.737	334.0	−10.05	0.986	1.804	138.6	3456.9
MS···Zn^{2+}	−169.56	1.815	327.1	−9.65	0.983	1.818	138.3	3510.5
MS···Mn^{+}	−90.35	1.634	340.4	−9.63	0.972	1.820	140.3	3662.2
MS···Co^{+}	−64.16	1.787	246.8	−9.43	0.973	1.827	139.7	3657.5
MS···Cu^{+}	−51.33	1.957	223.8	−9.90	0.972	1.812	140.0	3646.3

results reflect the interplay enhancement of both interactions. In other words, the stronger the noncovalent interactions, the more remarkable these effects; as a result, the complex with both strongest interactions should be the most energetically favorable.

Geometric descriptors

To provide more insight into the nature of noncovalent interactions, we have considered the most significant structural parameters, i.e., the distance between the ion and the center of the aromatic ring ($d_{\pi\ldots M}$) in the studied complexes. It is well known that the strength of the cation-π interaction increases with decreasing of the $d_{\pi\ldots M}$. According to the results presented in Table 1, the $d_{\pi\ldots M}$ in the MS complexes shows higher values than the BEN complexes. Based on these outcomes, the coexistence of the cation-π and IMHB interactions decreases the strength of the cation-π in the monovalent complexes. However, there is no a meaningful relationship between the computed $d_{\pi\ldots M}$ values and the achieved binding energies in the divalent ones (see Table 1). For monovalent complexes, the augmented $d_{\pi\ldots M}$ values, which are proportional to the type of cations, increase as follows: Mn^{+} (0.033) > Cu^{+} (0.027) > Co^{+} (0.020 Å).

We also intend to investigate how the cation-π interaction affects the IMHB strength of the resulting structures. For this purpose, we have analyzed the structural parameters of RAHB units, which are the most important indicators of the HB strength. As it is apparent from Fig. 1, the studied complexes represent one O–H···O IMHB in its structure. The formation of O–H···O HB is accompanied with the lengthening of O–H bond, the shortening of H···O distance, and the increase of the O–H···O angle. The values of geometrical parameters are given in Table 1. As shown in this table, the parent molecule creates the shorter H···O distance ($d_{H\cdots O}$) and the greater O–H···O angle (θ_{OHO}) in comparison with the corresponding values of the MS complexes (with the exception of π···Ni^{2+} complex). Alternatively, the O–H bond length ($d_{O\text{-}H}$) in the parent molecule is also less than the MS complexes value. The reason for the increase of the $d_{O\text{-}H}$ and $d_{O\ldots H}$ during the formation of complexes can be due to the electrostatic effects between metal ions and oxygen atom of the carbonyl functional group connected to the phenyl ring. There is the large negative charge on the oxygen atom (e.g., − 1.061 for Mn^{+} complex), which causes the oxygen atom to transfer a certain amount of electron density towards the metal ion. Thus, it leads to increasing the bond lengths in the related complexes.

According to these results, it is evident from Table 1 that the presence of cation-π interaction decreases the strength of the IMHB. The result of calculations also shows that the trend in the obtained $d_{H\cdots O}$ values is MS···Co^{+} (1.827) > MS···Mn^{+} (1.820) > MS···Cu^{+} (1.812 Å) and MS···Zn^{2+} (1.818) > MS···Fe^{2+}(1.804) > MS (1.803) > MS···Ni^{2+}(1.703 Å). There is a linear relationship between values of the E_{HB} and the $d_{H\ldots O}$ with an excellent correlation coefficient (R^2 is equal to 0.9974), while the corresponding correlation cannot be seen for the $d_{O\,H}$ values. In other words, our studies show that the $d_{O\ldots H}$ values correlate better with the E_{HB} than the $d_{O\text{-}H}$ ones. On the other hand, the $d_{O\text{-}H}$ values increase in the following order, MS···Ni^{2+} (0.998) > MS···Fe^{2+} (0.986) > MS···Zn^{2+} (0.983 Å) and MS···Co^{+} (0.973) > MS···Mn^{+}(0.972) ≈ MS···Cu^{+}(0.972) > MS (0.967 Å), that have good correlation with the binding energies (see Fig. 2).

Spectroscopic descriptors

In order to analyze the interplay between the cation-π and IMHB interactions, the most important stretching frequencies ($\nu_{\pi\cdots M}$) computed at the M06-2X/aug-cc-pVTZ level of theory are listed in Table 1. The strength of cation-π interactions

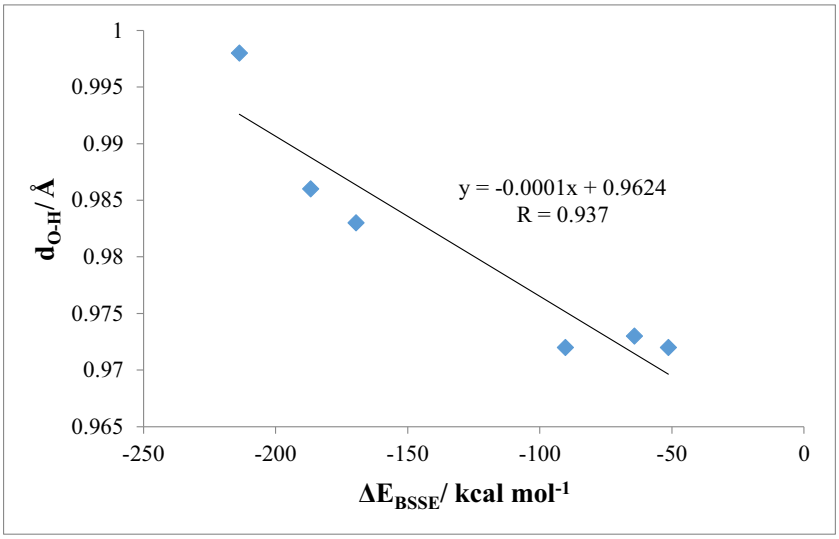

Fig. 2 The relationship between the values of d_{O-H} and ΔE_{BSSE}

can be evaluated using the $\nu_{\pi\cdots M}$. In other words, the calculations reveal a direct relationship between the calculated vibrational frequencies and the binding energies for the studied complexes. It is apparent from Table 1 that the changes in $\nu_{\pi\cdots M}$ values are in the ranges of 217.1–329.9 and 223.8–347.6 cm^{1} for BEN···M and MS···M complexes, respectively. Our data show that these values for MS complexes are higher than the corresponding values for BEN complexes. The increased values can be arranged, respectively, as Ni^{2+} (45.6) > Zn^{2+} (22.6) > Fe^{2+} (9.6 cm^{1}) and Mn^{+} (10.5) > Cu^{+}(6.7) > Co^{+}(5.0 cm^{1}); as a result, the increasing of $\nu_{\pi\cdots M}$ values and the strengthening of cation-π interaction can be observed in the presence of IMHB.

The O–H stretching mode (ν_{O-H}) is the most significant vibrational mode of O–H···O unit, in which its wave number strongly depends on the IMHB strength (see Table 1). For the parent molecule, there is a reverse relationship between the O–H bond length (d_{O-H}) and its corresponding frequency (ν_{O-H}). In other words, the O–H stretching vibrational frequency is observed to shift to a higher frequency, together with a contraction of the O–H bond (see Table 1). As shown in this table, the cation-π interaction reduces the values of ν_{O-H} in the studied complexes. It is evident from the conventional definition of HB that formation of X–H···Y bond is accompanied by a weakening and elongation of the covalent X–H bond with concomitant decrease of X–H stretching frequency [55]. The lengthening of the proton donating bond as an effect of HB formation is accompanied by the red shift of the corresponding mode. Hence, the ν_{O-H} values show red-shifted nature for the MS complexes. In comparison with the parent molecule, the ν_{O-H} for the MS complexes appears red-shifted by ca. Ni^{2+} (532.6) > Fe^{2+} (289.9) > Zn^{2+}(236.3 cm^{1}) and Cu^{+}(100.5) > Co^{+}(89.3) > Mn^{+} (84.6 cm^{1}), which is in good agreement with the E_{HB} and $d_{O\,H}$ (related to divalent complexes).

Topological descriptors

The mutual effects between the cation π and IMHB interactions can also be investigated by the topological properties of the bond critical points of interactions. The computed topological parameters of complexes such as charge density (ρ), its Laplacian ($\nabla^2\rho$), the total electron energy density (H_C), and its components (G_C, kinetic electron energy density, and V_C, potential electron energy density) at the bond critical points (BCPs) are given in Table 2. Figure 3 shows the typical molecular graphs obtained from AIM analysis for MS···Mn^{+} and BEN···Mn^{+} complexes. As observed in this figure, the bond paths are detected between metal cations and each carbon atom of the benzene ring in the related complexes.

It is well known that the value of ρ at the BCP ($\rho(r)_{\pi\cdots M}$) reflects the strength of cation-π interaction, with low values corresponding to weak interactions, and the ρ value enhances as the strength of interaction increases [56]. The theoretical results display that the presence of RAHB unit increases the $\rho(r)_{\pi\cdots M}$ values for the title complexes with respect to BEN···M. Hence, the augment of $\rho(r)_{\pi\cdots M}$ for the MS complexes in comparison with the BEN ones is found to be in the order Ni^{2+} (1.375×10^{2}) > Fe^{2+} (0.262×10^{2}) > Zn^{2+} (0.247×10^{2}a.u.) and Cu^{+} (0.563×10^{2}) > Mn^{+} (0.521×10^{2}) > Co^{+} (0.259×10^{2} a.u.). This means that the effect of the RAHB units on the $\rho(r)_{\pi\cdots M}$ values depends on the type of the cation; as a result, the coexistence of the IMHB and cation-π interactions increases the strength of cation-π interaction in the related complexes.

Based on AIM analysis, the topological properties of the electron density at the BCP of HB ($\rho(r)_{H\cdots O}$) are a criterion for evaluating the HB strength. Table 2 demonstrates the calculated topological parameters at the HB critical points. As shown in this table, the trend in the obtained $\rho(r)_{H\cdots O}$ values is as follows:

Table 2 The selected topological properties of electron density (a.u. × 10^2 except −G/V) obtained by AIM analysis

	π···M						HB				
	n	ρ(r)	$\nabla^2\rho(r)$	H(r)	V(r)	−G/V	ρ(r)	$\nabla^2\rho(r)$	H(r)	V(r)	-G/V
BEN···Ni^{2+}	2	6.527	12.358	−2.008	−7.106	0.717	—	—	—	—	—
BEN···Fe^{2+}	6	6.462	20.442	−1.284	−7.678	0.833	—	—	—	—	—
BEN···Zn^{2+}	6	5.007	13.319	−0.843	−5.016	0.832	—	—	—	—	—
BEN···Mn^{+}	6	7.062	28.360	−1.101	−9.292	0.882	—	—	—	—	—
BEN···Co^{+}	2	5.547	21.481	−0.526	−6.423	0.918	—	—	—	—	—
BEN···Cu^{+}	6	3.925	12.641	−0.248	−3.656	0.932	—	—	—	—	—
MS	—	—	—	—	—	—	3.488	12.897	0.006	−3.213	1.002
MS···Ni^{2+}	2	7.902	15.385	−2.896	−9.638	0.700	4.447	14.399	−0.403	−4.405	0.909
MS···Fe^{2+}	1	6.724	20.609	−1.475	−8.103	0.818	3.486	12.776	−0.003	−3.201	0.999
MS···Zn^{2+}	3	5.254	14.459	−0.911	−5.437	0.832	3.371	12.621	0.042	−3.072	1.014
MS···Mn^{+}	2	7.583	24.473	−1.861	−9.840	0.811	3.325	13.103	0.105	−3.066	1.034
MS···Co^{+}	1	5.806	20.627	−0.781	−6.719	0.884	3.277	12.906	0.112	−3.002	1.037
MS···Cu^{+}	1	4.488	14.311	−0.435	−4.447	0.902	3.393	13.346	0.091	−3.154	1.029

$MS\cdots Ni^{2+}$ $(4.447 \times 10^{-2}) > MS\cdots Fe^{2+}$ $(3.486 \times 10^{-2}) > MS\cdots Zn^{2+}$ $(3.371 \times 10^{-2}$a.u.) and $MS\cdots Cu^{+}$ $(3.393 \times 10^{-2}) > MS\cdots Mn^{+}$ $(3.325 \times 10^{-2}) > MS\cdots Co^{+}$ $(3.277 \times 10^{-2}$a.u.). Our theoretical results show that this trend is identical with the E_{HB} parameters (Tables 1 and 2). According to the obtained $\rho(r)_{H\cdots O}$ value for the parent molecule (3.488×10^{-2}a.u.), with the exception of Ni^{2+}complex, the presence of cation-π interaction decreases the IMHB strength in the studied complexes.

The $-G_C/V_C$ ratio can also treat as a descriptor for evaluating of the noncovalent interactions nature [57, 58]: for $-G_C/V_C > 1$, the interaction is electrostatic, while for $0.5 < -G_C/V_C < 1$, it is partly covalent. Table 2 shows that at the BCP of the HB, the ratio of $-G/V_{H\cdots O}$ for Ni^{2+} and Fe^{2+} complexes is between 0.5 and 1, which show that the IMHB is partly covalent in nature, while the remainder ones are electrostatic. On the other hand, the obtained $-G/V_{\pi\cdots M}$ values (ranging from 0.700 to 0.932) also confirm that the cation-π interactions in the systems under consideration are partly covalent.

Charge transfer descriptors

The NBO method encompasses a suite of algorithms that enable fundamental bonding concepts to be extracted from DFT computations [59]. One can see that the most significant donor–acceptor interaction in the considered complexes is $\sigma_{C-C} \rightarrow LP^*_M$ interaction. The results of NBO analysis indicate that the σ_{C-C} of the benzene ring acts as donor and the LP^*_M behaves as an acceptor. The obtained outcomes for the NBO analyses are reported in Table 3. As revealed in this table, the presence of IMHB increases the energies of $\sigma_{C-C} \rightarrow LP^*_M$ interaction. In other words, the coexistence of the cation-π and IMHB interactions enhances the strength of cation-π interactions. For instance, the augmented value of these interactions ($E^{(2)}$) for $MS\cdots Ni^{2+}$ complex is about 0.24 kcal mol^{-1} in comparison with the corresponding value of the $BEN\cdots Ni^{2+}$. According to the obtained $E^{(2)}$energies, these values depend on the type of cation and obey the π···

Fig. 3 Typical molecular graphs obtained from AIM analysis for (**a**) MS···Mn^{+} and (**b**) BEN···Mn^{+} complexes. The small red and yellow spheres and lines correspond to bond critical points (BCPs), ring critical points (RCPs), and bond paths, respectively

Table 3 The values of $E^{(2)}$ correspond to $\sigma_{(C-C)} \rightarrow LP^*_{(M)}$ and $LP_{(O)} \rightarrow \sigma^*_{(O-H)}$ interactions (in kcal mol^{-1}) and occupation numbers of donor (ON_D) and acceptor (ON_A) orbitals in the studied complexes

	π···M interaction			HB interaction		
	$\sigma_{(C-C)} \rightarrow LP^*_{(M)}$			$LP_{(O)} \rightarrow \sigma^*_{(O-H)}$		
	$E^{(2)}$	$ON_{\sigma(C-C)}$	$ON_{LP^*(M)}$	$E^{(2)}$	$ON_{LP(O)}$	$ON_{\sigma^*(O-H)}$
BEN···Ni^{2+}	4.46	1.984	0.075	–	–	–
BEN···Fe^{2+}	6.38	1.975	0.375	–	–	–
BEN···Zn^{2+}	3.31	1.979	0.013	–	–	–
BEN···Mn^{+}	7.27	1.966	0.055	–	–	–
BEN···Co^{+}	5.15	1.973	0.197	–	–	–
BEN···Cu^{+}	4.15	1.980	0.053	–	–	–
MS	–	–	–	10.13	1.953	0.024
MS···Ni^{2+}	4.70	1.975	0.011	17.90	1.934	0.045
MS···Fe^{2+}	8.08	1.964	0.081	10.42	1.945	0.030
MS···Zn^{2+}	3.87	1.976	0.014	9.74	1.947	0.028
MS···Mn^{+}	7.62	1.957	0.026	8.80	1.951	0.025
MS···Co^{+}	6.12	1.970	0.203	8.67	1.951	0.024
MS···Cu^{+}	5.55	1.979	0.054	9.24	1.950	0.025

$Fe^{2+} > \pi\cdots Ni^{2+} > \pi\cdots Zn^{2+}$ and $\pi\cdots Mn^{+} > \pi\cdots Co^{+} > \pi\cdots Cu^{+}$ order.

The NBO analysis also offers a method for exploring intramolecular bonding and charge transfer in molecular structures [43]. The NBO results show that the main orbital interaction in the O–H···O IMHB is $LP_{(O)} \rightarrow \sigma^*_{(O\text{-}H)}$. The lone pairs of oxygen (LP_O) participates as proton acceptor, and antibonding orbital of O–H ($\sigma^*_{O\text{-}H}$) has role of proton donor. The obtained data are listed in Table 3. The results of the NBO analysis indicate that the coupling of the cation-π and IMHB interactions decreases the IMHB strength (except for Ni^{2+} and Fe^{2+} complexes). However, it can be seen that the order of the $E^{(2)}$ values is as follows: MS···Ni^{2+} > MS···Fe^{2+} > MS···Zn^{2+} and MS···Cu^{+} > MS···Mn^{+} > MS···Co^{+}. These values depend on the type of cations involved in the interaction.

Electronic descriptors

Another important criterion to evaluate the interplay effects between the cation π and IMHB interactions is the electronic properties of complexes based on the frontier molecular orbital (FMO) theory. The highest occupied molecular orbital (HOMO) is the highest amount of energy orbital that can simply be donated electron density to form a bond, and the lowest unoccupied molecular orbital (LUMO) is the lowest empty orbital that energetically could add more electrons into this orbital. The chemical activity of complexes can be characterized by the energy gap (E_g) that is a significant parameter relying on the HOMO and LUMO energy levels. A case from the plots of HOMO and LUMO for the studied complexes is shown in Fig. 4.

The electronic descriptors of reactivity in the context of DFT such as energy gap, softness (S), chemical hardness (η), electronic chemical potential (μ), electrophilicity index (ω), and electronegativity (χ) are presented in Table 4. The large E_g means a hard molecule, and the small E_g means a soft molecule. In addition, the stability of the molecule with the most E_g can be related to hardness. This means that the molecule with the least E_g is more reactive. It is also obvious from Table 4 that the μ values of complexes are negative; hence, all the considered structures are stable. The μ presents a technique to compute the χ values for atoms and molecules. The μ is known as the negative of the χ. It is well known that the complexes with the higher χ value are better electron acceptors. The ω demonstrates that a good electrophile is a species described by a high |μ| value and a low η value [60]. There is a direct relationship between the minimum E_g and the maximum electron flow among HOMO and LUMO.

It is obvious from Table 4 that the presence of RAHB rings reduces the E_g, η, and χ descriptors and enhances the values of S, μ, and ω (in most cases) in comparison with BEN complexes. A similar trend is also observed for these parameters in the presence of cation-π interactions (except for χ and μ). In other words, it can be stated that the coexistence of the IMHB and cation-π interactions decreases the E_g, η, and μ parameters and increases the S, χ, and ω values with respect to parent molecule. The reduction of the E_g and η in MS complexes is due to the low chemical stability and high chemical reactivity of these complexes with respect to BEN ones. Hence, it can be concluded that, in most cases, both cation-π and HB interactions have same trend for these descriptors. This means that

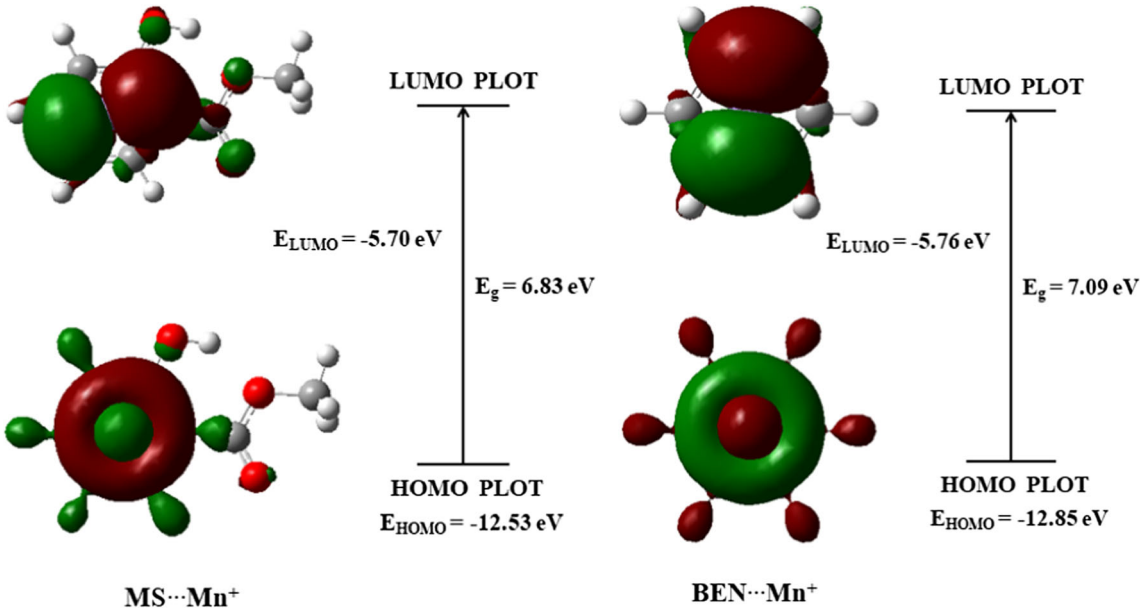

Fig. 4 HOMO and LUMO of MS···Mn^+ and BEN···Mn^+ complexes as obtained at the M06-2X/aug-cc-pVTZ level of theory

the cation-π interaction has a similar effect on the HB interaction and vice versa.

The high chemical reactivity of MS complexes with respect to BEN ones can also be evaluated by another index. Among reactivity descriptors, the molecular electrostatic potential (MEP) is a real property to analyze the physical nature of the noncovalent interactions involved in the complexes. It has especially been applied as a reliable descriptor for the HB strength [61–64]. The negative regions of MEP are related to electrophilic reactivity, and the positive regions are related to nucleophilic reactivity. Figure 5 shows electron density isosurface mapped with electrostatic potential surface for Mn^+ complexes. As can be seen, while the regions having the positive potential are over Mn^+ cation and plane of the benzene ring (blue color), the regions having the negative potential are over the oxygen atoms (red and yellow colors). The negative regions lead to strong electrostatic interactions with HB donors [61, 62, 65]. Therefore, the most negative sections of MEP that correspond to the lone-pair regions of the oxygen atoms in the complexes represent a measure of HB ability.

Conclusions

The interplay among the cation-π and IMHB interactions involving aromatic ring is studied by means of DFT calculations

Table 4 Values of the HOMO and LUMO energies (E_{HOMO}, E_{LUMO}), energy gap (E_g), chemical hardness (η), softness (S), electronic chemical potential (μ), electronegativity (χ), and electrophilicity index (ω)

	E_{HOMO} (eV)	E_{LUMO} (eV)	E_g (eV)	η (eV)	S (eV^{-1})	μ (eV)	χ (eV)	ω (eV)
BEN···Ni^{2+}	−19.699	−14.154	5.545	2.773	0.180	−16.926	16.926	51.666
BEN···Fe^{2+}	−20.598	−12.547	8.051	4.026	0.124	−16.572	16.572	34.111
BEN···Zn^{2+}	−19.943	−13.528	6.415	3.207	0.156	−16.736	16.736	43.664
BEN···Mn^+	−12.851	−5.759	7.092	3.546	0.141	−9.305	9.305	12.208
BEN···Co^+	−12.907	−5.786	7.121	3.561	0.140	−9.346	9.346	12.267
BEN···Cu^+	−13.724	−6.175	7.550	3.775	0.132	−9.950	9.950	13.112
MS	−7.927	−0.648	7.279	3.639	0.137	−4.288	4.288	2.526
MS···Ni^{2+}	−18.193	−12.996	5.197	2.599	0.192	−15.595	15.595	46.791
MS···Fe^{2+}	−18.232	−11.837	6.395	3.198	0.156	−15.034	15.034	35.343
MS···Zn^{2+}	−18.083	−12.996	5.087	2.544	0.197	−15.540	15.540	47.469
MS···Mn^+	−12.532	−5.701	6.830	3.415	0.146	−9.117	9.117	12.168
MS···Co^+	−12.477	−5.738	6.740	3.370	0.148	−9.108	9.108	12.308
MS···Cu^+	−12.705	−6.122	6.583	3.291	0.152	−9.413	9.413	13.461

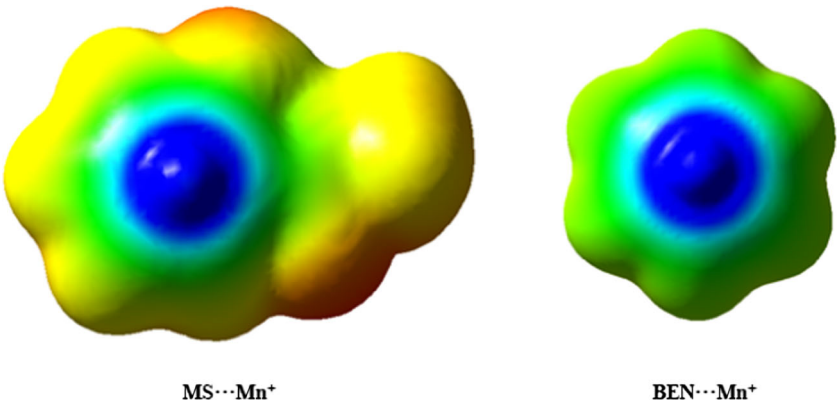

Fig. 5 Electron density isosurface for MS···Mn^+ and BEN···Mn^+ complexes calculated by M06-2X method and aug-cc-pVTZ basis set

on complexes of MS with Mn^+, Fe^{2+}, Co^+, Ni^{2+}, Cu^+, and Zn^{2+} cations. These outcomes are compared with the corresponding results of BEN···M complexes and the parent molecule as a set of reference points. The energetic, geometrical, spectroscopic, topological, and molecular orbital descriptors are applied to evaluate the strength of these interactions. Based on the energetic conclusions, for the double-charge cations, the simultaneous presence of these interactions enhances the strength of the cation-π, while for the mono-charge cations, the reverse process is observed. In contrast to the energetic conclusions, for both type of the cations (mono- and divalent), the descriptors of geometrical, spectroscopic, and AIM and NBO analyses indicate that the coupling simultaneously strengthens the cation-π interaction and weakens the strength of the IMHB in the studied systems (with the exception of Ni^{2+} complex). Our findings also show that, in most cases, both cation-π and HB interactions have the same trend for the electronic descriptors of reactivity. This means that the cation-π interaction has a similar effect on the HB interaction and vice versa.

Acknowledgments The support of this work by Vali-e-Asr University of Rafsanjan is acknowledged.

Authors' contributions M. P. is a graduate student who prepared the complexes and worked on the structures under direct supervision of M. M.; A. K. is an advisor, and M. M. wrote the manuscript.

Data availability From corresponding authors upon request.

Compliance with ethical standards

Not applicable. The ethical standards have been met.

Conflict of interest The authors declare that they have no conflict of interest.

Code availability Gaussian 03 Revision-B.01-SMP.

References

1. Gerhartz W (1985) Ullmann's encyclopedia of industrial chemistry. VCH, Hoboken
2. Carson JL, Willett LR (1993) Toxicity of nonsteroidal anti-inflammatory drugs. An overview of the epidemiological evidence. Drugs 46:243–248. https://doi.org/10.2165/00003495-199300461-00063
3. Mason L, Moore RA, Edwards JE, McQuay HJ, Derry S, Wiffen PJ (2004) Systematic review of efficacy of topical rubefacients containing salicylates for the treatment of acute and chronic pain. BMJ 328:995. https://doi.org/10.1136/bmj.38040.607141.EE
4. Vaile JH, Davis P (1998) Topical NSAIDs for musculoskeletal conditions. A review of the literature. Drugs 56:783–799. https://doi.org/10.2165/00003495-199856050-00004
5. Meyer EA, Castellano RK, Diederich F (2003) Interactions with aromatic rings in chemical and biological recognition. Angew Chem Int Ed 42:1210–1250. https://doi.org/10.1002/anie.200390319
6. Dougherty DA (1996) Cation-π interactions in chemistry and biology: a new view of benzene, Phe, Tyr, and Trp. Science 271:163–168. https://doi.org/10.1126/science.271.5246.163
7. Kim KS, Tarakeshwar P, Lee JY (2000) Molecular clusters of π-systems: theoretical studies of structures, spectra, and origin of interaction energies. Chem Rev 100:4145–4186. https://doi.org/10.1021/cr990051i
8. Lee EC, Kim D, Juree'ka P, Tarakeshwar P, Hobza P, Kim KS (2007) Understanding of assembly phenomena by aromatic–aromatic interactions: benzene dimer and the substituted systems. J Phys Chem A 111:3446–3457. https://doi.org/10.1021/jp068635t
9. Reddy AS, Sastry GN (2005) Cation [M = H^+, Li^+, Na^+, K^+, Ca^{2+}, Mg^{2+}, NH_4^+, and NMe_4^+] interactions with the aromatic motifs of naturally occurring amino acids: a theoretical study. J Phys Chem A 109:8893–8903. https://doi.org/10.1021/jp0525179
10. E'erný J, Hobza P (2007) Non-covalent interactions in biomacromolecules. Phys Chem Chem Phys 9:5291–5303. https://doi.org/10.1039/B704781A
11. Jeffrey GA, Saenger W (1991) Hydrogen bonding in biology and chemistry. Springer-Verlag, Berlin
12. Jeffrey GA (1997) An introduction to hydrogen bonding. Oxford University Press, New York
13. Desiraju GR, Steiner T (1999) The weak hydrogen bond in structural chemistry and biology. Oxford University Press, Oxford
14. Scheiner S (1997) Hydrogen bonding. A Theoretical Perspective. Oxford University Press, Oxford
15. Pauling L (1960) The nature of the chemical bond. Cornell University Press, Ithaca, New York
16. Buckingham AD, Legon AC, Roberts SM (1993) Principles of molecular recognition. Blackie Academic & Professional, London
17. Gilli G, Belluci F, Ferretti V, Bertolasi V (1989) Evidence for resonance-assisted hydrogen bonding from crystal-structure correlations on the enol form of the .beta.-diketone fragment. J Am Chem Soc 111:1023–1028. https://doi.org/10.1021/ja00185a035

18. Cubero E, Luque FJ, Orozco M (1998) Is polarization important in cation–π interactions? Proc Natl Acad Sci 95:5976–5980. https://doi.org/10.1073/pnas.95.11.5976
19. Ma JC, Dougherty DA (1997) The Cation−π interaction. Chem Rev 97:1303–1324. https://doi.org/10.1021/cr9603744
20. Schneider HJ (1991) Mechanisms of molecular recognition: investigations of organic host–guest complexes. Angew Chem Int Ed Eng 30:1417–1436. https://doi.org/10.1002/anie.199114171
21. Hong BH, Bae SC, Lee CW, Jeong S, Kim KS (2001) Ultrathin single-crystalline silver nanowire arrays formed in an ambient solution phase. Science 294:348–351. https://doi.org/10.1126/science.1062126
22. Choi HS, Suh SB, Cho SJ, Kim KS (1998) Ionophores and receptors using cation-π interactions: collarenes. Proc Natl Acad Sci U S A 95:12094–12099. https://doi.org/10.1073/pnas.95.21.12094
23. Kim D, Tarakeshwar P, Kim KS (2004) Theoretical investigations of anion−π interactions: the role of anions and the nature of π systems. J Phys Chem A 108:1250–1258. https://doi.org/10.1021/jp037631a
24. Kim D, Hu S, Tarakeshwar P, Kim KS (2003) Cation−π interactions: a theoretical investigation of the interaction of metallic and organic cations with alkenes, arenes, and heteroarenes. J Phys Chem A 107:1228–1238. https://doi.org/10.1021/jp0224214
25. Hong BH, Lee JY, Lee CW, Kim JC, Bae SC, Kim KS (2001) Self-assembled arrays of organic nanotubes with infinitely long one-dimensional H-bond chains. J Am Chem Soc 123:10748–10749. https://doi.org/10.1021/ja016526g
26. Kim KS, Lee JY, Ha TK, Kim DH (1994) On binding forces between aromatic ring and quaternary ammonium compound. J Am Chem Soc 116:7399–7400. https://doi.org/10.1021/ja00095a050
27. Hunter CA, Sanders JKM (1990) The nature of π-π interactions. J Am Chem Soc 112:5525–5534. https://doi.org/10.1021/ja00170a016
28. Guo H, Salahub DR (1998) Cooperative hydrogen bonding and enzyme catalysis. Angew Chem Int Ed 37:2985–2990. https://doi.org/10.1002/(SICI)1521-3773(19981116)37:21<2985::AID-ANIE2985>3.0.CO;2-8
29. Estarellas C, Escudero D, Frontera A, Quiñonero D, Deyá PM (2009) Theoretical ab initio study of the interplay between hydrogen bonding, cation–π and π–π interactions. Theor Chem Accounts 122:325–332. https://doi.org/10.1007/s00214-009-0517-0
30. Estarellas C, Frontera F, Quiñonero D, Deyá PM (2009) Interplay between cation–π and hydrogen bonding interactions: are non-additivity effects additive? Chem Phys Lett 479:316–320. https://doi.org/10.1016/j.cplett.2009.08.035
31. Escudero D, Frontera A, Quiñonero D, Deyá PM (2008) Interplay between cation-π and hydrogen bonding interactions. Chem Phys Lett 456:257–261. https://doi.org/10.1016/j.cplett.2008.03.028
32. Vijay D, Zipse H, Narahari Sastry G (2008) On the cooperativity of cation-π and hydrogen bonding interactions. J Phys Chem B 112:8863–8867. https://doi.org/10.1021/jp804219e
33. Li Q, Li W, Cheng J, Gong B, Sun J (2008) Effect of methyl group on the cooperativity between cation–π interaction and NH···O hydrogen bonding. J Mol Struct 867:107–110. https://doi.org/10.1016/j.theochem.2008.07.031
34. Zakian VA (1995) Telomeres: beginning to understand the end. Science 270:1601–1607. https://doi.org/10.1126/science.270.5242.1601
35. Rooman M, Lievin J, Bulsine E, Wintjens R (2002) Cation–π/H-bond stair motifs at protein–DNA interfaces. J Mol Biol 319:67–76. https://doi.org/10.1016/s0022-2836(02)00263-2
36. Frisch MJ, Trucks GW, Schlegel HB, Scuseria GE, Robb MA, Cheeseman JR, Zakrzewski VG, Montgomery JA, Stratmann JRE, Burant JC, Dapprich S, Millam JM, Daniels AD, Kudin KN, Strain MC, Farkas O, Tomasi J, Barone V, Cossi M, Cammi R, Mennucci B, Pomelli C, Adamo C, Clifford S, Ochterski J, Petersson GA, Ayala PY, Cui Q, Morokuma K, Malick DK, Rabuck AD, Raghavachari K, Foresman JB, Cioslowski J, Ortiz JV, Stefanov BB, Liu G, Liashenko A, Piskorz P, Komaromi I, Gomperts R, Martin RL, Fox DJ, Keith T, Al-Laham MA, Peng CY, Nanayakkara A, Gonzalez C, Challacombe M, Gill PMW, Johnson B, Chen W, Wong MW, Andres JL, Gonzalez C, HeadGordon M, Replogle ES, Pople JA (2003) Gaussian 03, revision B.01. Gaussian, Inc, Pittsburgh
37. Zhao Y, Truhlar DG (2008) The M06 suite of density functionals for main group thermochemistry, thermochemical kinetics, noncovalent interactions, excited states, and transition elements. Theor Chem Accounts 120:215–241. https://doi.org/10.1007/s00214-007-0310-x
38. Frisch MJ, Pople JA, Binkley JS (1984) Self-consistent molecular orbital methods 25. Supplementary functions for Gaussian basis sets. J Chem Phys 80:3265–3269. https://doi.org/10.1063/1.447079
39. Boys SF, Bernardi F (1970) The calculation of small molecular interactions by the differences of separate total energies. Some procedures with reduced errors. Mol Phys 19:553–566. https://doi.org/10.1080/00268977000101561
40. Bader RFW (1990) Atoms in molecules: a quantum theory. Oxford University Press, New York
41. Biegler-König FW, Bader RFW, Tang TH (1982) Calculation of the average properties of atoms in molecules. II. J Comput Chem 3:317–328. https://doi.org/10.1002/jcc.540030306
42. Biegler-König FW, Schonbohm J, Derdan R, Bayles D, Bader R (2000) AIM2000, Version 2.000
43. Reed AE, Curtiss LA, Weinhold F (1988) Intermolecular interactions from a natural bond orbital, donor–acceptor viewpoint. Chem Rev 88:899–926. https://doi.org/10.1021/cr00088a005
44. Glendening ED, Reed AE, Carpenter JE, Weinhold F (1992) NBO, version 3.1. Gaussian Inc., Pittsburgh
45. Pearson RG (1997) Chemical hardness – applications from molecules to solids. Weinheim, VCH-Wiley
46. Chattaraj PK, Poddar A (1999) Molecular reactivity in the ground and excited electronic states through density-dependent local and global reactivity parameters. J Phys Chem A 103:8691–8699. https://doi.org/10.1021/jp991214+
47. Parr RG, Lv S, Liu S (1999) Electrophilicity index. J Am Chem Soc 121:1922–1924. https://doi.org/10.1021/ja983494x
48. Sen KD, Jorgensen CK (1987) Electronegativity, structure and bonding. Springer Verlag, New York
49. Koopmans T (1934) Uber die Zuordnung von Wellenfunktionen und Eigenwerten zu den einzelnen Elektronen eines atoms. Physica 1:104–113. https://doi.org/10.1016/S0031-8914(34)90011-2
50. Espinosa E, Molins E (2000) Retrieving interaction potentials from the topology of the electron density distribution: the case of hydrogen bonds. J Chem Phys 113:5686–5694. https://doi.org/10.1063/1.1290612
51. Espionsa E, Souhassou M, Lachekar H, Lecomte C (1999) Topological analysis of the electron density in hydrogen bonds. Acta Crystallogr B 55:563–572. https://doi.org/10.1107/s0108768199002128
52. Abramov YA (1997) On the possibility of kinetic energy density evaluation from the experimental electron-density distribution. Acta Crystallogr A 53:264–272. https://doi.org/10.1107/S010876739601495X
53. Palusiak M, Simon S, Sola M (2006) Interplay between intramolecular resonance-assisted hydrogen bonding and aromaticity in o-hydroxyaryl aldehydes. J Organomet Chem 71:5241–5248. https://doi.org/10.1021/jo060591x
54. Güell G, Poater J, Luis JM, Mó O, Yáñez M, Sola M (2005) Aromaticity analysis of lithium cation/π complexes of aromatic

systems. Chem Phys Chem 6:2552–2561. https://doi.org/10.1002/cphc.200500216
55. Steiner T (2002) The hydrogen bond in the solid state. Angew Chem Int Ed 41:48–76. https://doi.org/10.1002/1521-3773(20020104)41:1<48::AID-ANIE48>3.0.CO;2-U
56. Garau C, Frontera A, Quiñonero D, Ballester P, Costa A, Deyà PM (2004) Cation-π versus anion-π interactions: energetic, charge transfer, and aromatic aspects. J Phys Chem A 108:9423–9427. https://doi.org/10.1021/jp047534x
57. Parra RD, Ohlssen J (2008) Cooperativity in intramolecular bifurcated hydrogen bonds: an ab initio study. J Phys Chem A 112:3492–3498. https://doi.org/10.1021/jp711956u
58. Ziółkowski M, Grabowski SJ, Leszczynski J (2006) Cooperativity in hydrogen-bonded interactions: ab initio and "atoms in molecules" analyses. J Phys Chem A 110:6514–6521. https://doi.org/10.1021/jp060537k
59. Balachandran V, Nataraj A, Karthick T (2013) Molecular structure, spectroscopic (FT-IR, FT-Raman) studies and first-order molecular hyperpolarizabilities, HOMO–LUMO, NBO analysis of 2-hydroxy-p-toluic acid. Spectrochim Acta A Mol Biomol Spectrosc 104:114–129. https://doi.org/10.1016/j.saa.2012.11.052
60. Domingo LR, Ríos-Gutiérrez M, Pérez P (2016) Applications of the conceptual density functional theory indices to organic chemistry reactivity. Molecules 21:748(1–22). https://doi.org/10.3390/molecules21060748
61. Baeten A, Proft FD, Geerlings P (1995) Basicity of primary amines: a group properties based study of the importance of inductive (electronegativity and softness) and resonance effects. Chem Phys Lett 235:17–21. https://doi.org/10.1016/0009-2614(95)00084-H
62. Baeten A, Proft FD, Geerlings P (1996) Proton affinity of amino acids: their interpretation with density functional theory-based descriptors. Int J Quantum Chem 60:931–939. https://doi.org/10.1002/(SICI)1097-461X(1996)60:4<931::AID-QUA14>3.0.CO;2-7
63. Akher FB, Ebrahimi A (2015) π-Stacking effects on the hydrogen bonding capacity of methyl 2-naphthoate. J Mol Graph Model 61:115–122. https://doi.org/10.1016/j.jmgm.2015.06.013
64. Kushwaha PS, Mishra PC (2000) Relationship of hydrogen bonding energy with electrostatic and polarization energies and molecular electrostatic potentials for amino acids: an evaluation of the lock and key model. Int J Quantum Chem 76:700–713. https://doi.org/10.1002/(SICI)1097-461X(2000)76:6<700::AID-QUA3>3.0.CO;2-V
65. Mishra PC, Kumar A (1996) Molecular electrostatic potentials and fields: hydrogen bonding, recognition, reactivity and modeling. Theor Comput Chem 3:257–296. https://doi.org/10.1016/S1380-7323(96)80046-X